Nuclear Physics A552 (1993) 323–339
North-Holand

NUCLEAR
PHYSICS A

Escape and spreading widths of the isobaric analog states of Sn and Te isotopes

J. Jänecke
Department of Physics, University of Michigan, Ann Arbor, MI 48109, USA

J.A. Bordewijk and S.Y. van der Werf
Kernfysisch Versneller Instituut, Zernikelaan 25, 9747 AA Groningen, The Netherlands

M.N. Harakeh
Faculteit Natuurkunde en Sterrenkunde, Vrije Universiteit, de Boelelaan 1081, 1081 HV Amsterdam, The Netherlands

Received 3 April 1992

Abstract: The escape widths for direct proton decay from isobaric analog states in Sb and I nuclei have been obtained by combining calculated single-particle widths with experimental spectroscopic information for neutron pickup reactions on the respective Sn and Te target nuclei. They display a pronounced odd-A/even-A staggering effect with very small widths for the even-A isotopes due to the lower proton decay energies. Only data for odd-A nuclei are available, and there is good agreement. Combining the calculated escape widths with the known experimental total widths yields values for the spreading widths. As expected, and in agreement with theoretical predictions, the spreading widths are essentially constant and dependent only weakly on neutron excess. Interestingly, the spreading widths are independent of whether statistical isospin-violating neutron decay is energetically possible or not, as is the case for the isobaric analog states of the light Sn isotopes with $A<116$. The branching ratios for the isospin-forbidden neutron decays from the isobaric analog states average about 95% for the heavier even-A Sb isotopes, and about 60% for the odd-A isotopes. Gamma-ray deexcitation and direct and statistical proton decay compete in the decays of the IAS of the light Sn isotopes, and a branching ratio of about 90% for gamma-ray deexcitation is expected for the IAS in ^{112}Sb.

1. Introduction

The total widths Γ of isobaric analog states (IAS) which have lorentzian line shapes can be described as a sum of an escape width and a spreading width in accordance with the two main components in the IAS wave function.

The escape width $\Gamma^{\uparrow}$ is made up of a sum of partial decay widths which are due to the isospin-allowed proton decays to single-neutron hole states in the daughter nucleus. The partial decay widths are proportional to the single-particle widths [1]) which are strongly affected by the proton separation energies S_p and the Coulomb and centrifugal barriers. The other factors are the spectroscopic factors C^2S observed

in single-neutron pickup reactions on the parent nuclei. The widths $\Gamma^{\uparrow}$ are thus connected with basic spectroscopic information.

The spreading width $\Gamma^{\downarrow}$ is the result of isospin-violating contributions to the IAS wave function which usually make neutron decay possible. In lighter nuclei, these contributions are believed to result from mixing with configuration or anti-analog states and, in heavier nuclei, from mixing with the isovector giant monopole resonance [2]) (IVGMR). The width $\Gamma^{\downarrow}$ thus provides important information about isospin-violating processes, about the IVGMR, and about doorway states.

It is the purpose of the present work to report on calculations of the escape widths $\Gamma^{\uparrow}$ of the IAS for all Sn and Te isotopes, to establish their characteristics and to compare them to available data. The method outlined earlier [1]) was employed, and all available spectroscopic information for neutron pickup reactions was used for the calculations. Subsequently, the spreading widths $\Gamma^{\downarrow}$ were deduced using the known experimental total widths Γ. Here again, the characteristics were determined and compared to theoretical predictions. Attention was given to the decay modes associated with $\Gamma^{\downarrow}$. This aspect is important because isospin-forbidden neutron decay is not always energetically permitted.

2. Theoretical considerations

2.1. ESCAPE WIDTH $\Gamma^{\uparrow}$

The $T_>$ component of the IAS is obtained by operating with the isospin-lowering operator T_- on the parent-state wave function. It therefore consists of a coherent superposition of particle-hole excitations, and proton emission leads to single-neutron hole states. These are the same states reached in neutron pickup reactions on the parent nucleus. The close connection between the escape width $\Gamma^{\uparrow}$ and the respective neutron pickup spectroscopic factors C^2S can be expressed [1]) as a sum over the various hole states as

$$\Gamma^{\uparrow} = \sum_{jj} C^2 S_f(j) \frac{\Gamma^{\uparrow}_{\text{s.p.}}(j, E_p, E_n)}{(N-Z)}. \tag{1}$$

Here, E_n is the binding energy of the neutron which is transformed into a proton in the charge-exchange process, and E_p is the proton decay energy. The single-particle (proton) escape width $\Gamma^{\uparrow}_{\text{s.p.}}$ can be calculated from the square of the matrix element representing the overlap between the wave function of the bound neutron which is transformed and that of the decaying proton. The procedure consists of constructing the wave functions by varying the proton decay energy E_p near the IAS resonance and finding the depth of the Woods–Saxon potential well for each proton energy. The standard geometry with $r_0 = 1.25$ fm, $a = 0.65$ fm, $\lambda = 25$ has been used throughout. Subsequently the f.w.h.m. of the distribution for the square of this overlap integral is determined. It represents the single-particle escape width for the respective particle-hole configuration of the IAS.

A simpler expression for the single-particle escape width was reported earlier [3,4]). It consists of a product of a reduced width (Wigner limit) and a proton penetration factor calculated from Coulomb functions. Thus, $\Gamma^{\uparrow}$ of eq. (1) depends on the spectroscopic factors C^2S for neutron pickup, but it is also very sensitive to the proton separation energies and the angular momentum carried away by the decay proton on account of the Coulomb and centrifugal barriers.

2.2. SPREADING WIDTH $\Gamma^{\downarrow}$

The theoretical description [2,5]) of the spreading width $\Gamma^{\downarrow}$ in medium-heavy and heavy nuclei assumes isospin mixing via the charge-dependent Coulomb force between the IAS and the (T_0-1) component of the isovector giant monopole resonance (IVGMR). The latter then couples to underlying 2p2h doorway states with isospin $T_< = T_0-1$ via the strong residual interaction. Combining this description with a strength-function approach [6]) for the damping width of the IVGMR leads to

$$\Gamma^{\downarrow} = 2\pi V_{\mathrm{CD}}^2 S(E_{\mathrm{IAS}}) \tag{2}$$

with

$$S(E) = \frac{1}{2\pi} \frac{\Gamma_{\mathrm{IVGMR}}(E)}{(E-E_{\mathrm{IVGMR}})^2 + (\frac{1}{2}\Gamma_{\mathrm{IVGMR}}(E))^2}. \tag{3}$$

Here, V_{CD} is the charge-dependent matrix element coupling the IAS with the IVGMR, and the second factor represents the energy-dependent strength function $S(E)$ taken at $E = E_{\mathrm{IAS}}$. The quantity $\Gamma_{\mathrm{IVGMR}}(E)$, also to be taken at $E = E_{\mathrm{IAS}}$, represents the distribution of the coupling strength between the IVGMR and the doorway states. Eq. (2) did initially not give a satisfactory description of the available data. In particular, the observed strong increase with neutron excess for several sequences of deformed isotopes was not reproduced. However, acceptable agreement was obtained [7]) for the available data with $A > 110$, including the IAS of the Sn and Te isotopes, by postulating for deformed nuclei a splitting of the IVGMR strength due to mixing with the β-vibration component of the isovector giant quadrupole resonance (IVGQR). A similar splitting of the isoscalar quadrupole resonance and mixing with the isoscalar monopole resonance, and hence a significant shift of the monopole strength to lower excitations energies, is well established both theoretically and experimentally [8,9]).

3. Procedures and results

Calculating the escape widths $\Gamma^{\uparrow}$ from eq. (1) requires knowledge of experimental or calculated spectroscopic factors C^2S. These values are listed in table 1. Since the dominant contributions in the sum of eq. (1) come from $l = 0$ proton decay between 0^+ and $\frac{1}{2}^+$ states, pickup of $2s_{1/2}$ neutrons will provide the most important terms,

and only these C^2S are included in the table. Columns 5–8 and 10–13 give experimental spectroscopic factors C^2S for the transitions to the 0^+ or $\frac{1}{2}^+$ ground states or excited $\frac{1}{2}^+$ states, respectively. They are separately displayed for even-A and odd-A nuclei. Columns 5, 6 and 10, 11 show experimental values for the (p, d) and (d, t) neutron pickup reactions, respectively. The values in columns 7, 8 and 12, 13 are deduced from the spectroscopic factors for the (d, p) neutron stripping reaction on the neighboring neutron-deficient isotope.

The spectroscopic factors C^2S of table 1 are displayed in fig. 1 as function of neutron number N for both, the Sn and the Te targets. Spectroscopic factors from the (p, d) neutron pickup reaction are given in columns 5 and 10. Special attention was given to the data of Cavanagh *et al.* [10]) who measured this reaction for all stable even-A Sn targets including angular distributions for the lowest $s_{1/2}$ states but do not report spectroscopic factors. An analysis of these data by us using well established optical-model parameters [11,12]) provides reliable relative spectroscopic factors. Absolute values can only be based on the reported cross sections at $\theta = 6°$ where the $l = 0$ angular distributions have steep slopes. Since the finite opening angle of the spectrograph may have a significant effect on the effective angle, it was decided to renormalize the relative values by a factor 0.5 to obtain $C^2S = 0.41$ for ^{116}Sn in agreement with reanalyzed (d, t) data [13]). The values so obtained are shown in fig. 1 as filled squares. A few additional values from other (p, d) data are included as filled small circles. The latter are treated as secondary data input.

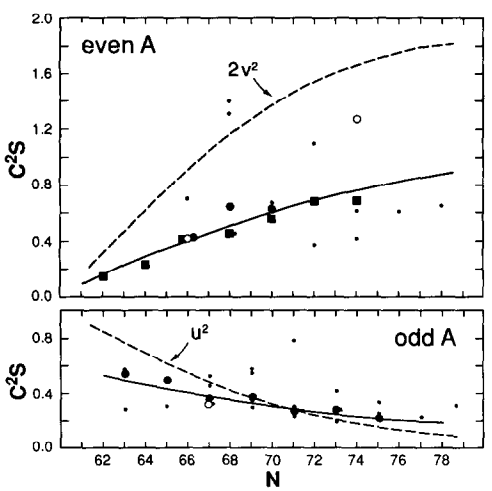

Fig. 1. Spectroscopic factors C^2S for $2s_{1/2}$ neutron pickup, for even-A (top) and odd-A (bottom) Sn and Te isotopes. Primary data (open and filled circles and squares) and secondary data (filled small circles) are taken from table 1. The solid curves represent the adopted values used for the calculations (see text). The dashed curves represent limits based on BCS occupation probabilities (see text).

Spectroscopic factors C^2S from the (d, t) neutron pickup reaction of columns 6 and 11 are included in fig. 1 as open circles [13-15]) and filled small circles, respectively.

The values listed in columns 7 and 12 are deduced from one single complete set of (d, p) data measured by Schneid *et al.* [16]). These data were reanalyzed by us using both, the original optical-model parameters and more recent parameter sets [11,12]). A radial cutoff employed originally was not used. The standard geometry for generating the bound-state wave functions of the transferred neutrons was introduced. The reanalyzed spectroscopic factors C^2S deviate by up to factors of two from the originally reported values. The C^2S so obtained are shown in fig. 1 as filled circles.

Additional spectroscopic factors C^2S deduced from other (d, p) data of columns 8 and 13 are also included in fig. 1 as filled small circles. The uncertainties for these data points are difficult to estimate because of the use of differing parameter sets. They may exceed a factor of two in some cases.

Table 1 contains in column 14 additional values for C^2S which were derived from the experimental magnetic moments μ of the respective $J^\pi = \frac{1}{2}^+$ ground states. By using the ^{117}Sn(d, t)^{116}Sn, Schippers *et al.* [14]) demonstrated that $\mu(^{117}\mathrm{Sn})$ is largely determined by the $s_{1/2}$ strength. Neglecting small contributions from states with $J^\pi = 1^+$, the approximate result

$$\sum_f C^2S(0_f^+) \approx -0.523\, \mu(\tfrac{1}{2}^+)/\mu_N \tag{4}$$

was found in good agreement with the experimentally observed $s_{1/2}$ strengths $C^2S(0_f^+)$ for the neutron pickup reaction to the neighboring even-A isotope. Assuming a constant fraction of $C^2S(0^+_{g.s.})/\sum C^2S(0^+)$ for the $s_{1/2}$ strength residing in the ground state, as found [14]) in ^{116}Sn(d, t), one obtains the estimate

$$C^2S(0^+_{g.s.}) \approx -0.322\, \mu(\tfrac{1}{2}^+)/\mu_N\,. \tag{5}$$

This equation was used to obtain the values in column 14 of table 1 for several odd-A nuclei. They are also shown in fig. 1 as filled small circles.

Complete and consistent sets of estimated values for $C^2S(\mathrm{g.s.}; 2s_{1/2})$ for the Sn and Te isotopes are shown in columns 9 and 15, and they are represented by solid lines in fig. 1. As described in the next section, they are based on the experimental values, but considerations related to the fullness or emptiness of the $2s_{1/2}$ orbital in the respective initial or final 0^+ ground states for even-A or odd-A targets are also considered.

The next column 16 gives the calculated single-particle escape widths $\Gamma^{\uparrow}_{s.p.}$ divided by the neutron excess $(N-Z)$. A very pronounced odd-A/even-A staggering is already apparent from the calculated values. As mentioned before in sect. 2.1. they were obtained from the square of an overlap integral. The input energies at which the partial s-wave shifts take on the value $\frac{1}{2}\pi$ have been shifted slightly to values which place the maxima of the distributions to the appropriate proton decay energies. This increases the singe-particle widths by as much as 12%.

TABLE 1

Experimental and estimated spectroscopic factors for neutron pickup reactions and (d, p) stripping reactions on Sn and Te isotopes. Calculated single-particle escape widths $\Gamma^{\uparrow}_{s.p.}$ and escape widths $\Gamma^{\uparrow}$ for the IAS of the Sn and Te isotopes

(1)	(2)	(3)	(4)	(5)	(6)	(7)	(8)	(9)
				$C^2S(2s_{1/2}$; even $A)$				
Nuclei	A	J^{π}	E_x (keV)	exp. (p, d)	exp. (d, t)	exp. (d, p)	exp. (d, p)	adopted
Sn-Sb	112	0^+	0	0.145 [a]				0.160
	113	$\frac{1}{2}^+$	0					
	114	0^+	0	0.230 [a]				0.285
	115	$\frac{1}{2}^+$	0					
	116	0^+	0	0.410 [a], 0.7 [b]	0.41 [d]	0.42 [j]		0.400
	117	$\frac{1}{2}^+$	0					
	118	0^+	0	0.445 [a], 1.4 [c]	1.31 [e]	0.64 [j]	0.449 [k]	0.505
	119	$\frac{1}{2}^+$	0					
	120	0^+	0	0.550 [a]		0.62 [j]		0.600
	121	$\frac{1}{2}^+$	60					
	122	0^+	0	0.680 [a]				0.685
	123	$\frac{1}{2}^+$	150					
	124	0^+	0	0.685 [a]	1.27 [f]			0.760
	125	$\frac{1}{2}^+$	215					
Te-I	121	$\frac{1}{2}^+$	0					
	122	0^+	0		0.67 [g]			0.600
	123	$\frac{1}{2}^+$	0					
	124	0^+	0		1.10 [h]		0.37 [l]	0.685
	125	$\frac{1}{2}^+$	0					
	126	0^+	0		0.41 [i]		0.62 [m]	0.760
	127	$\frac{1}{2}^+$	61					
	128	0^+	0		0.61 [i]			0.825
	129	$\frac{1}{2}^+$	181					
	130	0^+	0		0.65 [i]			0.880
	131	$\frac{1}{2}^+$	296					

[a]) See ref. [10]); reanalyzed; normalization factor 0.5; see text. [b]) Ref. [27]). [c]) Ref. [28]). [d]) Ref. [13]). [e]) Ref. [29]). [f]) Ref. [15]). [g]) Ref. [30]). [h]) Ref. [31]). [i]) Ref. [32]). [j]) Ref. [16]); reanalyzed. [k]) Ref. [33]). [l]) Ref. [34]). [m]) Ref. [35]).

According to eq. (1), the main contribution to the escape width $\Gamma^{\uparrow}$ are obtained by multiplying these $2s_{1/2}$ single-particle widths by the respective spectroscopic factors C^2S. These values are expected to approximately describe the experimental escape widths subject to the reliability of the spectroscopic factors. The contributions of proton decays to excited states are further expected to lead to small increases for the combined total escape widths due to the summation over the transitions to all states as required by eq. (1). Indeed, using the detailed and reliable spectroscopic data for ground and excited transitions for the reactions ^{116,117}Sn(d, t) ^{115,116}Sn

TABLE 1—continued

(10)	(11)	(12)	(13)	(14)	(15)	(16)	(17)	(18)	(19)
		$C^2S(2s_{1/2}$; odd $A)$				$\Gamma^{\uparrow}_{s.p.}(2s_{1/2})/(N-Z)$	$\Gamma^{\uparrow}(2s_{1/2})$	$\Gamma^{\uparrow}$	$\Gamma^{\uparrow}$
exp. (p, d)	exp. (d, t)	exp. (d, p)	exp. (d, p)	exp. μ	adopted	calc. (keV)	calc. (keV)	calc. (keV)	calc. (keV)
						0.07			0.01 ± 0.01
		0.54 [j])	0.57 [g])	0.28 [aa])	0.491	28.0			14.7 ± 2.2
						0.21			0.08 ± 0.02
		0.49 [j])		0.30 [aa])	0.430	30.0			13.3 ± 2.0
						1.09	0.58 ± 0.09	0.75 ± 0.11	0.56 ± 0.17
0.45 [n])	0.32 [p])	0.36 [j])	0.52 [r])	0.32 [aa])	0.375	43.0	13.8 ± 2.1	14.8 ± 2.2	17.2 ± 2.6
						1.24			0.81 ± 0.24
0.55 [d])		0.37 [j])	0.29 [s])	0.34 [aa])	0.327	53.0			18.8 ± 2.8
						1.74			1.35 ± 0.40
		0.27 [j])	0.30 [t])		0.285	61.9			18.9 ± 2.8
						2.38			2.10 ± 1.05
		0.28 [j])	0.19 [e])		0.249	67.9			18.1 ± 2.7
						2.98			2.92 ± 1.46
		0.22 [j])	0.33 [u])		0.220	76.4			18.0 ± 2.7
			0.58 [i])		0.327	33.7			11.8 ± 1.8
						0.78			0.60 ± 0.18
			0.78 [v])	0.24 [aa])	0.285	41.0			12.6 ± 1.9
						1.37			1.21 ± 0.60
			0.42 [w])	0.28 [aa])	0.249	49.0			12.9 ± 1.9
						2.13			2.09 ± 1.05
			0.25 [x])		0.220	55.7			13.1 ± 2.0
						2.88			3.06 ± 1.53
			0.22 [y])		0.197	61.8			13.0 ± 2.0
						3.73			4.24 ± 2.12
			0.31 [z])		0.181	66.4			12.9 ± 1.9

[n]) Ref. [36]). [o]) Ref. [37]). [p]) Ref. [14]). [q]) Ref. [38]). [r]) Ref. [39]). [s]) Ref. [40]). [t]) Ref. [41]). [u]) Ref. [42]). [v]) Ref. [43]). [w]) Ref. [44]). [x]) Ref. [45]). [y]) Ref. [46]). [z]) Ref. [47]). [aa]) Estimated from magnetic moments; see text.

[refs. [13,14])] and the respective calculations for all single-particle escape widths for excited states leads to small increases in the total escape widths. Column 17 gives the calculated escape widths $\Gamma^{\uparrow}(2s_{1/2})$ based on $C^2S = 0.41$ and 0.32, respectively, from refs. [13,14]). Column 18 gives the combined widths $\Gamma^{\uparrow}$ which include all contributions from decays to excited states with lower proton decay energies and higher or the same l-values. Only two to three states give modest contributions. For ^{116}Sn and ^{117}Sn the increases are by factors of 1.29 and 1.08, respectively. An uncertainty of $\pm 15\%$ is assigned to these results. The calculated escape width $\Gamma^{\uparrow} = 14.8 \pm 2.2$ keV

for the IAS in ^{117}Sb is in very good agreement with the experimental value of $\Gamma^{\uparrow} = 16.5 \pm 3.3$ keV. In the absence of more detailed spectroscopic information for excited states, the above enhancement factors will be used below to account for decays to excited states for all even-A and odd-A nuclei.

Column 19, finally, gives the escape widths derived from the adopted values C^2S $(2s_{1/2})$ of columns 9 and 15, the calculated single-particle widths of column 16, and the above small enhancement factors. Uncertainties of ±30% are assigned to the even-A cases (±50% for $N \geq 72$) and ±15% to the odd-A cases. These uncertainties prove quite appropriate (see sect. 4).

Experimental and calculated total, escape and spreading widths for the IAS of all Sn and Te isotopes are listed in table 2. In addition the table gives the closely related branching ratios. The ground states of the light odd-A Sn and Te isotopes have $J^{\pi} = \frac{1}{2}^{+}$ based on the $2s_{1/2}$ orbital. These states become low-lying $\frac{1}{2}^{+}$ states in the heavier odd-A isotopes. The respective excitation energies are given in column 4. Also included in the table is experimental information for low-lying $\frac{3}{2}^{+}$ states.

Column 5 shows the experimental total widths Γ observed in (^{3}He, t) charge exchange [17]) and in proton resonance work [18,19]), respectively. The former data were obtained for all even-A isotopes as well as ^{117,119}Sn and ^{125}Te. The latter data were obtained for all odd-A isotopes. There is good agreement between the results from the two types of measurements, and averaged values are given for the three odd-A cases.

The only other available experimental data are the escape widths $\Gamma^{\uparrow}$ for odd-A nuclei obtained in proton resonance work [18,19]). They are given in column 6. Further included in this table in column 7 are the calculated values from table 1. The experimental and calculated escape widths are displayed in fig. 2a.

Spreading widths $\Gamma^{\downarrow}$ deduced from $\Gamma^{\downarrow} = \Gamma - \Gamma^{\uparrow}$ are listed in columns 8 and 9. The experimental total widths Γ of column 5 were used in both cases, and possible systematic errors will therefore affect both sets. Column 8 uses the available experimental values of $\Gamma^{\uparrow}$ from column 6. It includes a few widths for $\frac{3}{2}^{+}$ states. Column 9 uses the calculated values from column 7, and they therefore represent combined experimental/calculated values. Column 10 gives theoretical spreading widths $\Gamma^{\downarrow}$ from ref. [7]). They make use of the charge-dependent sum-rule matrix elements of Lane and Mekjian [20]), a parameterization of the excitation energies of the IVGMR, and a strength-function approach [6]). The postulated coupling [7]) with the IVGQR is included in the results.

The last four columns 11 to 14 show the experimental and calculated branching ratios $P^{\uparrow} = \Gamma^{\uparrow}/\Gamma$ and $P^{\downarrow} = \Gamma^{\downarrow}/\Gamma$. These branching ratios represent the relative decay probabilities for direct proton decay and, if energetically allowed, mostly statistical isospin-forbidden neutron decay. The various decay modes will be discussed in more detail in the next section.

All values in table 2 related to $\frac{3}{2}^{+}$ states in the heavier odd-A Sn and Te isotopes are given in parentheses.

TABLE 2

Experimental and calculated total, escape and spreading widths, Γ, $\Gamma^{\uparrow}$ and $\Gamma^{\downarrow}$, of the isobaric analog states of the Sn and Te isotopes. Experimental information for $\frac{3}{2}^{+}$ states is included and is given in parentheses

(1) Nuclei	(2) A	(3) J^{π}	(4) E_x (keV)	(5) Γ exp. [a,b]) (keV)	(6) $\Gamma^{\uparrow}$ exp. [b]) (keV)	(7) $\Gamma^{\uparrow}$ calc. [c]) (keV)	(8) $\Gamma^{\downarrow}$ exp. [b]) (keV)	(9) $\Gamma^{\downarrow}$ calc. [c]) (keV)	(10) $\Gamma^{\downarrow}$ theor. [d]) (keV)	(11) $P^{\uparrow}$ exp. [b]) (%)	(12) $P^{\uparrow}$ calc. [c]) (%)	(13) $P^{\downarrow}$ exp. [b]) (%)	(14) $P^{\downarrow}$ calc. [c]) (%)
Sn-Sb	112	0^{+}	0	26.0±9.0		0.01±0.01		25.99±9.00	25.9		0.0±0.0		100.0±0.0
	113	$\frac{1}{2}^{+}$	0	40.1±8.0	10.3±2.1	14.7±2.2	29.8±8.3	25.39±8.30	26.6	25.7±7.3	36.7±9.2	63.3±9.2	63.3±9.2
	114	0^{+}	0	10.0±9.0		0.08±0.02		9.92±9.00	27.2		0.8±0.7		99.2±0.7
	115	$\frac{1}{2}^{+}$	0	38.0±7.6	8.0±1.6	13.3±2.0	30.0±7.8	24.69±7.86	27.8	21.1±6.0	35.0±9.8	78.9±6.0	65.0±9.8
	116	0^{+}	0	34.0±9.0		0.56±0.17		33.44±9.00	28.3		1.6±0.7		98.4±0.7
	117	$\frac{1}{2}^{+}$	0	40.1±6.1	16.5±3.3	17.2±2.6	23.6±6.9	22.92±6.62	28.8	41.1±10.3	42.8±9.2	58.9±10.3	57.2±9.2
	118	0^{+}	0	26.0±9.0		0.81±0.24		25.19±9.00	29.2		3.1±1.4		96.9±1.4
	119	$\frac{1}{2}^{+}$	0	43.9±6.7	17.0±3.4	18.8±2.8	26.9±7.5	25.08±7.27	29.6	38.7±9.7	42.9±9.2	61.3±9.7	57.1±9.2
	120	0^{+}	0	32.0±9.0		1.35±0.40		30.65±9.01	29.9		4.2±1.7		95.8±1.7
	121	$\frac{3}{2}^{+}$	0	(39.0±7.8)	(7.5±1.5)		(31.5±7.9)			(19.2±5.4)		(80.8±5.4)	
		$\frac{1}{2}^{+}$	60	60.0±12.0	24.0±4.8	18.9±2.8	36.0±12.9	41.12±12.33	30.2	40.0±11.3	31.5±7.9	60.0±11.3	68.5±7.9
	122	0^{+}	0	35.0±9.0		2.10±1.05		32.90±9.06	30.5		6.0±3.4		94.0±3.4
	123	$\frac{3}{2}^{+}$	25	(42.0±8.4)	(7.0±1.4)		(35.0±8.5)			(16.7±4.7)		(83.3±4.7)	
		$\frac{1}{2}^{+}$	150	59.0±11.8	17.0±3.4	18.1±2.7	42.0±12.3	40.92±12.11	30.7	28.8±8.1	30.6±7.7	71.2±8.1	69.4±7.7
	124	0^{+}	0	33.0±9.0		2.92±1.46		30.08±9.12	30.8		8.9±5.0		91.1±5.0
	125	$\frac{3}{2}^{+}$	28	(57.0±11.4)	(9.0±1.8)		(48.0±11.5)			(15.8±4.5)		(84.2±4.5)	
		$\frac{1}{2}^{+}$	215	45.0±9.0	14.0±2.8	18.0±2.7	31.0±9.4	27.01±9.40	30.8	31.1±8.8	40.0±10.0	68.9±8.8	60.0±10.0
Te-I	121	$\frac{1}{2}^{+}$	0			11.8±1.8			37.1				
	122	0^{+}	0			0.60±0.18			36.6				
	123	$\frac{1}{2}^{+}$	0			12.6±1.9			36.1				
	124	0^{+}	0	22.0±9.0		1.21±0.60		20.79±9.02	35.7		5.5±3.5		94.5±3.5
	125	$\frac{1}{2}^{+}$	0	47.0±6.4	12.2±2.4	12.9±1.9	34.8±6.8	34.13±6.68	35.3	26.0±6.2	27.4±5.6	74.0±6.2	72.6±5.6
		$\frac{3}{2}^{+}$	35	(38.0±7.6)	(4.8±1.0)		(33.2±7.7)			(12.6±3.6)		(87.4±3.6)	
	126	0^{+}	0	24.0±9.0		2.09±1.05		21.91±9.06	35.0		8.7±5.5		91.3±5.5
	127	$\frac{3}{2}^{+}$	0	(43.2±8.6)	(5.7±1.1)		(37.5±8.7)			(13.2±3.7)		(86.8±3.7)	
		$\frac{1}{2}^{+}$	61	48.2±9.6	13.7±2.7	13.1±2.0	34.5±10.0	35.09±9.80	34.7	28.4±8.0	27.2±6.8	71.6±8.0	72.8±6.8
	128	0^{+}	0	22.0±9.0		3.06±1.53		18.94±9.13	34.5		13.9±9.0		86.1±9.0
	129	$\frac{3}{2}^{+}$	0	(51.0±10.2)	(6.2±1.2)		(44.8±10.3)			(12.2±3.4)		(87.8±3.4)	
		$\frac{1}{2}^{+}$	181	48.0±9.6	9.9±2.0	13.0±2.0	38.1±9.8	34.97±9.80	34.3	20.6±5.9	27.1±6.8	79.4±5.9	72.9±6.8
	130	0^{+}	0	37.0±9.0		4.24±2.12		32.76±9.25	34.2		11.5±6.4		88.5±6.4
	131	$\frac{3}{2}^{+}$	0	(77.0±15.4)	(8.5±1.7)		(68.5±15.5)			(11.0±3.1)		(89.0±3.1)	
		$\frac{1}{2}^{+}$	296	60.0±12.0	10.2±2.0	12.9±1.9	49.8±12.2	47.14±12.15	34.1	17.0±4.8	21.4±5.4	83.0±4.8	78.6±0.54

[a]) Ref. [17]). [b]) Refs. [18,19]). [c]) This work. [d]) Ref. [7]).

4. Discussion

Insight into the characteristics of the spectroscopic factors C^2S for $2s_{1/2}$ pickup reactions on the Sn and Te isotopes can be obtained by considering the summed strength $\sum_f C^2S(2s_{1/2})$ for all $2s_{1/2}$ transitions. These summed strengths represent limits for the quantities of interest and provide information about the expected trends.

Ignoring the fragmentation of strength, the 0^+ ground states of the even-A isotopes are assumed to be represented by BCS wave functions where the $2s_{1/2}$ components are described by the respective BCS fullness and emptiness parameters, $v(2s_{1/2})$ and $u(2s_{1/2})$. Furthermore, the $\frac{1}{2}^+$ (mostly) ground states of the odd-A isotopes are assumed to be one-quasi-particle (1qp) states which carry the full $2s_{1/2}$ 1qp strength. Other 1qp shell-model contributions are blocked.

Under these assumptions, spectroscopic factors C^2S are obtained from the fullness and emptiness parameters as

$$C^2S(0^+ \to \tfrac{1}{2}^+) = 2v^2(2s_{1/2}) \tag{6}$$

for even-A targets. Here, $v(2s_{1/2})$ is the fullness parameter of the even-A target nucleus. Correspondingly,

$$C^2S(\tfrac{1}{2}^+ \to 0^+) = u^2(2s_{1/2}) \tag{7}$$

for odd-A targets. Here, $u(2s_{1/2})$ is the emptiness parameter of the neighboring neutron-deficient even-A isotope. The sumrule strengths for the two idealized cases are $2v^2(2s_{1/2})$ and 1, respectively.

Fig. 1 displays as dashed lines the spectroscopic factors so obtained as function of the neutron number N for even-A (top) and odd-A (bottom) nuclei. The lines represent reasonable averages deduced from theoretical [21,22]) and experimental [16,18,23]) occupation probabilities. The calculations have been carried out with both, random phase [21]) and Tamm-Dancoff [22]) approximations supported by experimental values from (d, p) stripping [16]) and (p, t) two-neutron pickup [23]) reactions. Values for Te isotopes [19]) are also considered for the higher neutron numbers. As pointed out earlier [19]), the occupation probabilities for Te and Sn isotopes are similar at the same neutron number. This assumption is supported by the data of table 1. The assumption is certainly not satisfied exactly, but it should be acceptable within our stated uncertainties.

Except for $N = 74$, all primary data shown in fig. 1 by open and filled circles and squares follow well-defined trends. These trends when expressed by a smooth empirical dependence on N are represented by the two solid curves. The respective adopted spectroscopic factors are listed in columns 9 and 15 of table 1. The secondary data represented in fig. 1 by the filled small circles follow the general trends but, as expected, they also display significant scatter.

The experimental spectroscopic factors approximated by the solid lines and the calculated values based on BCS occupation probabilities (dashed lines) are shown in fig. 1. They display very different characteristics for the even-A and odd-A

isotopes. Whereas the experimental values are typically only about 50% of the calculated values for the even-A nuclei, they are in much closer agreement for the odd-A nuclei. This behavior can be explained on the basis of two effects which change the idealized spectroscopic factors of eqs. (6) and (7). These effects are (i) the fragmentation of the $2s_{1/2}$ BCS strength in the 0^+ ground states of the even-A isotopes, and (ii) the reduction in the $\frac{1}{2}^+$ (mostly) ground states of the odd-A isotopes of the extreme 1qp strength of 100%.

Significant fragmentation of the $2s_{1/2}$ BCS strength in the 0^+ ground states of even-A nuclei has been observed in detailed investigations [11,12]) of ^{116,117}Sn(d, t)^{115,116}Sn neutron pickup. Here, the ground states carry only about 84% and 60% of the observed strength, respectively. Furthermore, appreciable fractions of the available strengths could not be located in the energy intervals investigated.

For odd-A nuclei it was reported in a theoretical study [24]) that the lowest $\frac{1}{2}^+$ states carry only about 90% of the projected 1qp strength. It was suggested, however, from an investigation of the ^{117}Sn(d, t)^{116}Sn neutron pickup reaction [14]) that the true ground state of ^{117}Sn may deviate even more from a pure 1qp state.

Both of these effects lead to a significant reduction of $C^2S(0^+ \rightarrow \frac{1}{2}^+)$ from the value of eq. (6) for even-A target nuclei. The observed reduction from fig. 1 is about 50%.

The situation for $C^2S(\frac{1}{2}^+ \rightarrow 0^+)$ for odd-A target nuclei is different. A reduction of the projected 1qp strength in the target nucleus will reduce both, $C^2S(\frac{1}{2}^+ \rightarrow 0^+)$ and the sumrule strength. However, fragmentation of the BCS occupation probability $v^2(2s_{1/2})$ in the final 0^+ ground state will increase $C^2S(\frac{1}{2}^+ \rightarrow 0^+)$ because of the increased emptiness. Consequently, the two effects can lead to a partial cancellation which seems to be observed in fig. 1.

A quantitative description of the two effects will not be attempted here. However, it appears that the departures from a pure 1qp description of the $\frac{1}{2}^+$ states must be significantly greater than predicted [24]) leading to admixtures of more complicated 3qp states, particularly in the light odd-A Sn isotopes, as was also suggested earlier [14]) from a study of ^{117}Sn.

The escape widths $\Gamma^\uparrow$ of column 7 in table 2 derived from these spectroscopic factors C^2S and the calculated single-particle escape widths $\Gamma^\uparrow_{\text{s.p.}}$ are in good agreement with the available experimental values for the odd-A nuclei of column 6. Only the calculated values for ^{113}Sn and ^{115}Sn are high and slightly outside the quoted uncertainties. This may suggest that the C^2S deduced from the magnetic moments should be given more weight. Alternatively, the experimental values [18]) could be low. The low isotopic abundances of the two target nuclei do not appear to be responsible, but it is conceivable that the interference between the observed resonant and Coulomb background amplitudes is influenced by the presence of statistical proton emission (see below) for these two proton resonance reactions [14]). However, the overall agreement between the calculated and experimental escape widths $\Gamma^\uparrow$ gives credence to the assumption that the predicted values for the even-A isotopes for which no data exist are also reliable.

The calculated and experimental values of $\Gamma^{\uparrow}$ are displayed in fig. 2a as function of A for the IAS of both, the Sn and Te isotopes. There is a pronounced oscillatory structure with very small widths for the even-A isotopes, particularly the light ones. This odd-A/even-A staggering is mostly due to the strong dependence of the single-particle reduced widths on the proton decay energies Q_p. This quantity is plotted in fig. 2c, and it displays a strong oscillatory behavior as well superimposed on a weak increase with A. The calculations showed a rapid increase of $\Gamma^{\uparrow}_{s.p.}$ by three orders of magnitude for a variation of Q_p from 3 to 8 MeV. This dependence is best understood in the simplified expression [3,4]) where $\Gamma^{\uparrow}_{s.p.}$ is expressed as product of the Wigner limit of the reduced single-particle proton width and the Coulomb penetrability $p_l = 2k_l F_l/(F_l^2 + G_l^2)$. The values for $\Gamma^{\uparrow}_{s.p.}$ reported earlier [3,4]) for several Sn isotopes are in fact very close to the ones of table 1(factor 2 to 3 larger). Whitten *et al.* [4]) already pointed out that $\Gamma^{\uparrow}$ for even-A isotopes should be small. This was adopted as $\Gamma^{\uparrow} \approx 0$ for all even-A Sn and Te isotopes in ref. [17]).

Combining the experimental or calculated escape widths $\Gamma^{\uparrow}$ with the experimental total width Γ of column 5 in table 2 leads to the experimental and calculated spreading widths $\Gamma^{\downarrow}$ of columns 8 and 9, also displayed in fig. 2b. These indirectly determined calculated and experimental values are in excellent agreement with each other. The widths are essentially constant with no apparent staggering effects except possibly for the Te isotopes. The good agreement for the odd-A Te isotopes may suggest low/high values for the experimental total widths Γ of the odd-A/even-A isotopes. It is of interest to note that the experimental values in column 8 reported for the $\frac{3}{2}^+$ states agree well with those for the $\frac{1}{2}^+$ and 0^+ states. The only apparent discrepancy is the calculated small value for ^{114}Sn. It results from a small total width observed in the ^{114}Sn(^{3}He,t)^{114}Sb charge-exchange reaction [17]). A systematic error in the measurement could be responsible for this on account of the low isotopic abundance of the target used. Alternatively, it might also have a physical origin associated with the ($1d_{5/2}$, $1g_{7/2}$) subshell closure [25]) in ^{114}Sn.

Included in fig. 2 are the theoretical values [7]) of column 10 in table 2. They display a very weak dependence on neutron excess and, except for ^{114}Sn, there is good agreement with the experimental and calculated values. The theoretical values would decrease by about 35% if the postulated [7]) mixing in the calculations with the IVGQR is removed leading to poorer agreement. However, the strongest influence of this mixing is not displayed for the Sn and Te isotopes but instead for the strongly deformed rare-earth nuclei where it accounts for the pronounced increase with neutron excess.

The oscillatory behavior of the escape widths $\Gamma^{\uparrow}$ and the smooth behavior of the spreading widths $\Gamma^{\downarrow}$ is also visible in the oscillations observed for the total widths. The above characteristics are also reflected in the branching ratios $P^{\uparrow}$ and $P^{\downarrow}$. For the lightest even-A Sn isotopes $P^{\uparrow} \approx 0$ and hence $P^{\downarrow} \approx 100\%$. The quantity $P^{\uparrow}$ increases slightly for the even-A isotopes with increasing A, particularly for the Te isotopes, and on the average $P^{\uparrow} \approx 5\%$ and $P^{\downarrow} \approx 95\%$. For the odd-$A$ isotopes the

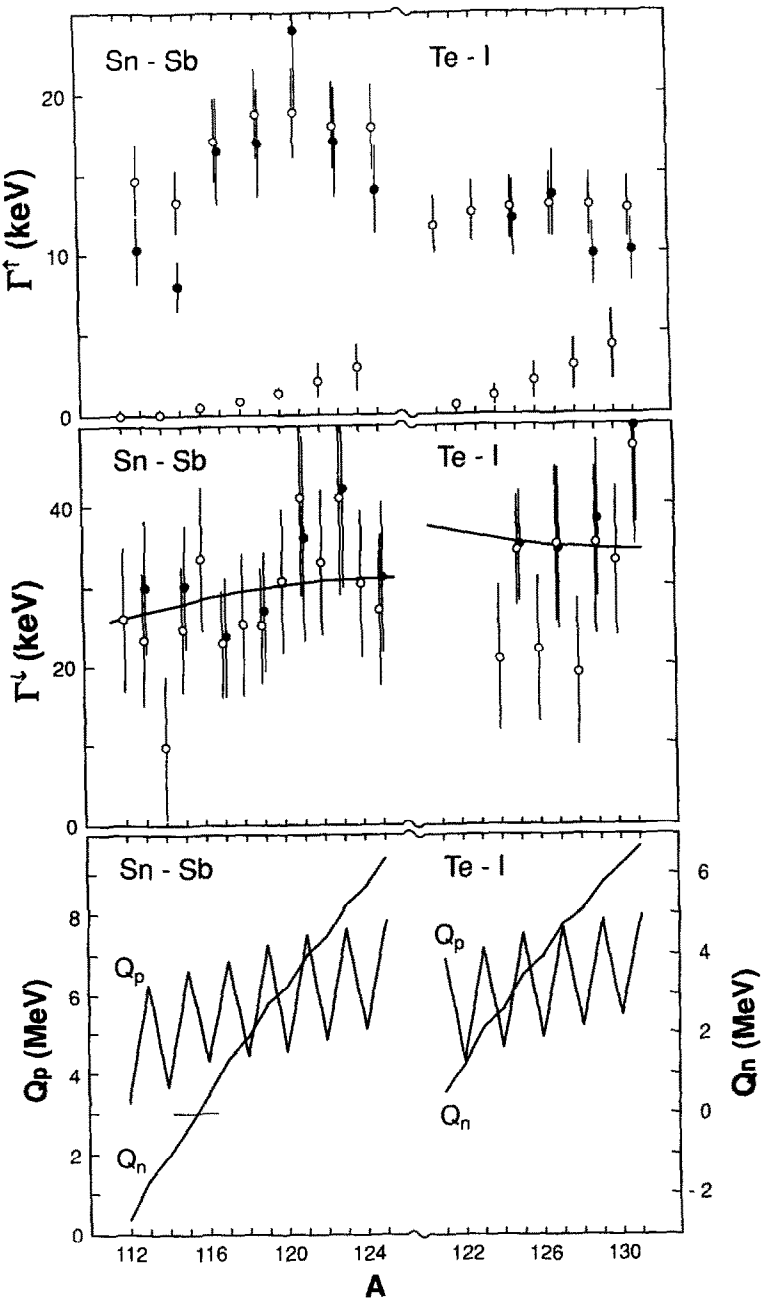

Fig. 2. Experimental (filled circles) and calculated (open circles) (a) escape widths $\Gamma^{\uparrow}$ and (b) spreading widths $\Gamma^{\downarrow}$ (including theoretical predictions) for the IAS of the Sn and Te isotopes. Part (c) shows the Q-values Q_p and Q_n for the direct proton decay and isospin-forbidden statistical neutron decay from the IAS to the respective ground states.

contributions from the escape width $\Gamma^{\uparrow}$ are not negligible, and the average values are $P^{\uparrow} \approx 30\%$ and $P^{\downarrow} \approx 70\%$.

The total width Γ determines the lifetime of an IAS. The IAS in ^{119}Sb, for example, has a lifetime $\tau \approx 1.5 \times 10^{-20}$ s with branching ratios $P^{\uparrow} \approx 40\%$ and $P^{\downarrow} \approx 60\%$. If one could "turn off" either "spreading" or "escape", then one would find $\tau^{\uparrow} \approx 3.7 \times 10^{-20}$ s and $\tau^{\downarrow} \approx 2.5 \times 10^{-20}$ s. The escape width $\Gamma^{\uparrow}$ leads to direct proton decay as noted above. However, the decay characteristics associated with the spreading width $\Gamma^{\downarrow}$ are not as clear. It is usually connected with isospin-forbidden statistical neutron decay. Indeed, calculations with the computer code CASCADE [26]) for the statistical emission of charged and neutral particles and gamma rays from the IAS in ^{119}Sb yield a probability of 93% for neutron emission.

However, the transition probabilities and penetrabilities for neutron emission are not the factors determining $\Gamma^{\downarrow}$. In fact, fig. 2c displays the Q-values for neutron emission to the ground states of the respective daughter nuclei. It shows that $Q_n < 0$ for the IAS in the Sb isotopes with $A < 116$ and neutron emission is therefore energetically not even possible. Calculations with the CASCADE code [26]) show that gamma-deexcitation and proton emission dominate the statistical decays for $A < 116$ reaching ~90% gamma deexcitation for $A = 112$. This contradicts earlier conclusions [3]) where $\Gamma_p/\Gamma = 1$ was assumed for the IAS of ^{91}Zr, ^{95}Mo and ^{115}Sn all of which have $Q_n < 0$.

The theoretical treatment of the spreading widths $\Gamma^{\downarrow}$ in heavier nuclei assumes mixing between the IAS and the IVGMR. It is described by eqs. (2) and (3). The charge-dependent matrix element V_{CD} connects the IAS and the IVGMR. Following this description [6]), the energy-dependent strength function $S(E)$ represents the distribution of the IVGMR wave function over the bound and continuum states of the nucleus. These are certain 2p2h doorway states (the "spreading state") which are coupled via the residual nuclear interaction to the collective 1p1h IVGMR state. It follows that the spreading width $\Gamma^{\downarrow}$ depends on the charge-dependent matrix element V_{CD}, on the nuclear matrix elements connecting the IVGMR and the doorway states, and on the density of doorway states near the IAS. The associated lifetime $\tau^{\downarrow} = 1/\Gamma^{\downarrow}$ therefore describes the time evolution of the spreading of the $T_> = T_0$ component of the 1p1h excitation populated in the charge-exchange reaction into 2p2h doorway states. It must compete with direct proton decay characterized by $\tau^{\uparrow} = 1/\Gamma^{\uparrow}$. The system subsequently progresses further towards a complete compound state which then decays into every open channel.

The decay characteristics of the IAS of the Sn isotopes shows interesting features which should be studied. Combining the calculated probabilities due to the escape and spreading widths from table 2 and the results for the statistical decays based on calculations with the CASCADE code [26]) leads to the results displayed in fig. 3. Here, the relative contributions from direct and statistical proton decay, statistical neutron decay and from γ-deexcitation are shown as bar diagrams as function of

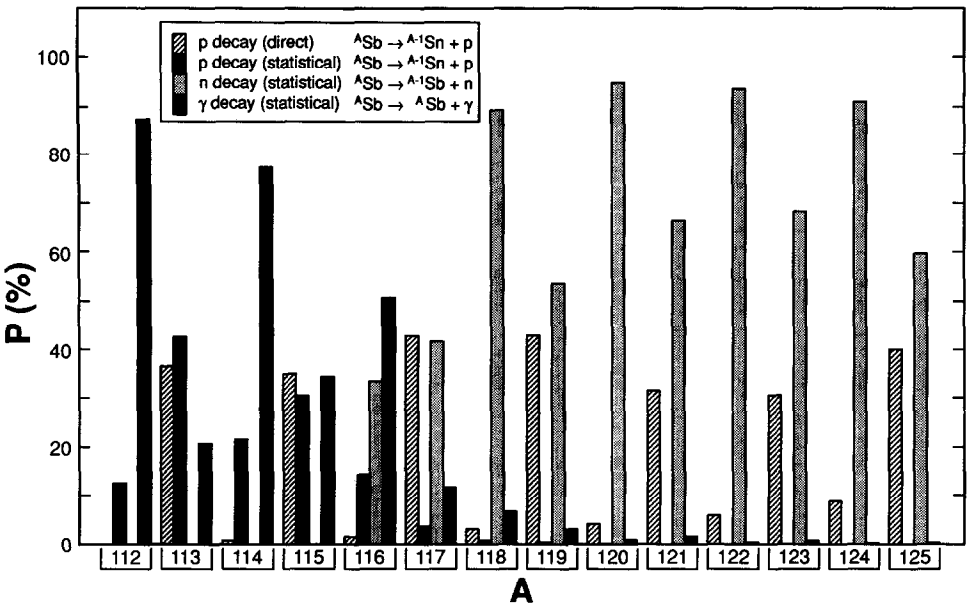

Fig. 3. Relative decay probabilities for direct and statistical proton decay, statistical neutron decay and γ-deexcitation from the IAS of the Sn isotopes.

A. Direct proton decay is given directly by the escape probabilities $P^{\uparrow}$ of table 2. The values alternate between small values from 0 to 7% for even A and values of about 40% for odd A. The balance is represented by neutron emission, but only for $A \geq 118$. For $A = 118$ to $A = 116$ contributions from γ-deexcitation and even statistical proton decay become important because of the increasing hindrance of neutron emission due to low decay energies (see fig. 2c). Neutron decay is not possible for $A < 116$, and a delicate balance between direct and statistical proton decay and γ-deexcitation develops influenced by the respective maximum decay energies. This includes ^{115}Sb where the three modes are predicted to be about equal, and ^{112}Sb which is expected to decay with ~90% probability by γ-emission. The multiplicity of γ-rays in the deexcitation is greater than unity which increases the total number of emitted γ-rays accordingly.

Discussions with K.T. Hecht are gratefully acknowledged. The research was supported in part by the National Science Foundation Grant PHY-8911831. This work was also part of the research program of the "Stichting voor Fundamenteel Onderzoek der Materie" (FOM) with financial support from the "Nederlandse Organisatie voor Wetenschappelijk Onderzoek" (NWO). Essential travel support by the Scientific Affairs Division, North Atlantic Treaty Organization, travel grant NATO 900219 is gratefully acknowledged.

References

1) S.Y. van der Werf, M.N. Harakeh and E.N.M. Quint, Phys. Lett. **B216** (1989) 15
2) A.Z. Mekjian, Nucl. Phys. **A146** (1970) 288
3) P.S. Miller and G.T. Garvey, Nucl. Phys. **A163** (1971) 65
4) C.A. Whitten, J. Chai, N. Chirapatpimol, W.H. Dunlop and G. Igo, Phys. Lett. **B51** (1974) 45
5) N. Auerbach, J. Hüfner, A.K. Kerman and C.M. Shakin, Rev. Mod. Phys. **44** (1972) 48
6) W.M. MacDonald and M.C. Birse, Phys. Rev. **C29** (1984) 425
7) J. Jänecke, M.N. Harakeh and S.Y. van der Werf, Nucl. Phys. **A463** (1987) 571
8) D. Zawischa, J. Speth and D. Pal, Nucl. Phys. **A311** (1978) 445;
   Y. Abgrall, B. Morand, E. Caurier and B. Grammaticos, Nucl. Phys. **A346** (1980) 431;
   S. Jang, Nucl. Phys. **A401** (1983) 303
9) M. Buenerd, D. Lebrun, Ph. Martin, P. de Saintignon and C. Perrin, Phys. Rev. Lett. **45** (1980) 1667;
   U. Garg, P. Bogucki, J.D. Bronson, Y.-W. Lui, C.M. Rozsa and D.H. Youngblood, Phys. Rev. Lett. **45** (1980) 1670;
   S. Brandenburg, R. De Leo, A.G. Drentje, M.N. Harakeh, H. Janszen and A. van der Woude, Phys. Rev. Lett. **49** (1982) 1687;
   H.P. Morsch, M. Rogge, P. Tureck, C. Mayer-Böricke and P. Decowski, Phys. Rev. **C25** (1982) 2939
10) P.E. Cavanagh, C.F. Coleman, A.G. Hardacre, G.A. Gard and J.F. Turner, Nucl. Phys. **A141** (1970) 97
11) F.D. Becchetti and G.W. Greenlees, Phys. Rev. **82** (1969) 1190
12) W.W. Daehnick, J.D. Childs and Z. Vrcelj, Phys. Rev. **C21** (1980) 2253
13) S.Y. van der Werf, M.N. Harakeh, L.W. Put, O. Scholten and R.H. Siemssen, Nucl. Phys. **A289** (1977) 141
14) J.M. Schippers, J.M. Schreuder, S.Y. van der Werf, K. Allaart, N. Blasi and M. Waroquier, Nucl. Phys. **A510** (1990) 70
15) W.T.A. Borghols, Ph.D. Thesis, University of Groningen (1988), unpublished
16) E. Schneid, A. Prakash and B.L. Cohen, Phys. Rev. **156** (1967) 1316
17) F.D. Becchetti, W.S. Gray, J. Jänecke, E.R. Sugarbaker and R.S. Tickle, Nucl. Phys. **A271** (1976) 77
18) P. Richard, C.F. Moore, J.A. Becker and J.D. Fox, Phys. Rev. **145** (1966) 971
19) J.L. Foster, P.J. Riley and C.F. Moore, Phys. Rev. **175** (1968) 1498
20) A.M. Lane and A.Z. Mekjian, Adv. Nucl. Phys. **7** (1973) 97
21) R. Arvieux and E. Salusti, Nucl. Phys. **66** (1965) 305
22) D.M. Clement and E.U. Baranger, Nucl. Phys. **A120** (1968) 25
23) D.G. Fleming, M. Blann, H.W. Fulbright and J.A. Robbins, Nucl. Phys. **A157** (1970) 1
24) G. Bonsigniori, M. Savoia, K. Allaart, A. Van Egmond and G. te Velde, Nucl. Phys. **A432** (1985) 389
25) J.H. Bjerregaard, O. Hansen, O. Nathan, R. Chapman and S. Hinds, Nucl. Phys. **131** (1969) 481
26) F. Pühlhofer, Nucl. Phys. **A280** (1977) 267;
   M.N. Harakeh, extended version (unpublished)
27) G. Berrier-Ronsin, G. Duhamel, E. Gerlic, J. Kalifa, H. Langevin-Joliot, G. Rotbard, M. Vergnes, J. Vernotte, K.K. Seth and K. Heyde, Nucl. Phys. **A288** (1977) 279
28) M. Sekiguchi, Y. Shida, F. Soga, Y. Hirao and M. Sakai, Nucl. Phys. **A278** (1977) 231
29) M. Sekiguchi, O. Hashimoto, Y., Shida and F. Soga, J. Phys. Soc. Jpn. **52** (1983) 1134
30) S. Gales, G.M. Crawley, D. Weber and B. Zwieglinski, Nucl. Phys. **A381** (1982) 173
31) M.A.G. Fernandes and M.N. Rao, J. of Phys. **G3** (1977) 1397
32) R.K. Jolly, Phys. Rev. **136** (1964) B683
33) E. Frota-Pessoa, Nuovo Cim. **77A** (1983) 369
34) J.R. Lien, C. Lunde Nilsen, R. Nilsen, P.B. Vold, A. Graue and G. Lovhoiden, Can. J. Phys. **55** (1977) 463
35) A. Graue, J.R. Lien, H. Vinje, P.B. Vold and W.M. Moore, Nucl. Phys. **A160** (1971) 497
36) K. Yagi, Y. Sayi, T. Ishimatsu, Y. Ishizaki, M. Matoba, Y. Nakayima and C.Y. Huang, Nucl. Phys. **A111** (1968) 129
37) D.G. Fleming, Can. J. Phys. **60** (1982) 428
38) T. Borello, Rev. Bras. Fis. **2** (1972) 157
39) P.L. Carson and L.C. McIntyre, Nucl. Phys. **A198** (1972) 289
40) T. Borello-Lewin, C.Q. Orsini, O. Dietzsch and E.W. Hamburger, Nucl. Phys. **A249** (1975) 284

41) M.J. Bechara and O. Dietzsch, Phys. Rev. **C12** (1975) 90
42) C.R. Bingham and D.L. Hills, Phys. Rev. **C8** (1973) 729
43) J.R. Lien, J.S. Vaagen and A. Graue, Nucl. Phys. **A253** (1975) 165
44) A. Graue, J.R. Lien, S. Royrvik, O.J. Aaroy and W.H. Moore, Nucl. Phys. **A136** (1969) 513
45) A. Graue, E. Hvidsten, J.R. Lien, G. Sandvik and W.H. Moore, Nucl. Phys. **A120** (1967) 493
46) W.H. Moore, G.K. Schlegel, S. O'Dell, A. Graue and J.R. Lien, Nucl. Phys. **A104** (1967) 327
47) A. Graue, E. Jastad, J.R. Lien, P. Torvund and W.H. Moore, Nucl. Phys. **A103** (1967) 209